



## ■ BONE BIOLOGY

# Intermittent parathyroid hormone increases stability and improves osseointegration of initially unstable implants

**K. Staats,  
B. R. Sosa,  
E-V. Kuyl,  
Y. Niu,  
V. Suhardi,  
K. Turajane,  
R. Windhager,  
M. B. Greenblatt,  
L. Ivashkiv,  
M. P. G. Bostrom,  
X. Yang**

From Hospital for  
Special Surgery, New  
York City, New York, USA

## Aims

To develop an early implant instability murine model and explore the use of intermittent parathyroid hormone (iPTH) treatment for initially unstable implants.

## Methods

3D-printed titanium implants were inserted into an oversized drill-hole in the tibiae of C57Bl/6 mice ( $n = 54$ ). After implantation, the mice were randomly divided into three treatment groups (phosphate buffered saline (PBS)-control, iPTH, and delayed iPTH). Radiological analysis, micro-CT ( $\mu$ CT), and biomechanical pull-out testing were performed to assess implant loosening, bone formation, and osseointegration. Peri-implant tissue formation and cellular composition were evaluated by histology.

## Results

iPTH reduced radiological signs of loosening and led to an increase in peri-implant bone formation over the course of four weeks (timepoints: one week, two weeks, and four weeks). Observational histological analysis shows that iPTH prohibits the progression of fibrosis. Delaying iPTH treatment until after onset of peri-implant fibrosis still resulted in enhanced osseointegration and implant stability. Despite initial instability, iPTH increased the mean pull-out strength of the implant from 8.41 N (SD 8.15) in the PBS-control group to 21.49 N (SD 10.45) and 23.68 N (SD 8.99) in the immediate and delayed iPTH groups, respectively. Immediate and delayed iPTH increased mean peri-implant bone volume fraction (BV/TV) to 0.46 (SD 0.07) and 0.34 (SD 0.10), respectively, compared to PBS-control mean BV/TV of 0.23 (SD 0.03) (PBS-control vs immediate iPTH,  $p < 0.001$ ; PBS-control vs delayed iPTH,  $p = 0.048$ ; immediate iPTH vs delayed iPTH,  $p = 0.111$ ).

## Conclusion

iPTH treatment mediated successful osseointegration and increased bone mechanical strength, despite initial implant instability. Clinically, this suggests that initially unstable implants may be osseointegrated with iPTH treatment.

**Cite this article:** *Bone Joint Res* 2022;11(5):260–269.

**Keywords:** Osseointegration, Aseptic loosening, Implant instability

## Article focus

- Early implant instability can dramatically impair long-term implant survival of arthroplasties.
- The aim of the study was to develop a murine model with unstable, uncemented tibial implants to analyze the therapeutic effect of intermittent parathyroid hormone (iPTH) treatment in terms

of osseointegration, implant stability, and peri-implant tissue formation.

## Key messages

- In this presented animal model, peri-implant tissue formation was similar to findings of loose uncemented implants in human patients.

Correspondence should be sent to  
Mathias P. G. Bostrom; email:  
BostromM@hss.edu

doi: 10.1302/2046-3758.115.BJR-2021-0489.R1

*Bone Joint Res* 2022;11(5):260–269.

- iPTH treatment of initial unstable implants leads to osseointegration and re-stabilization regarding pull-out strengths.
- Delayed iPTH is still capable of rescuing initial unstable implants and prohibiting fibrous tissue formation and increasing osseointegration.

### Strengths and limitations

- To our knowledge, this is the first study to evaluate implant instability in a murine model with weight-bearing conditions.
- iPTH treatment is able to enhance implant stability and rescue osseointegration failure in initially unstable conditions.
- Histological/immunohistochemistry data are only representative, not quantitative, and not performed with the implant in situ.

### Introduction

Early implant migration has been identified as a potential initial risk factor for aseptic loosening.<sup>1</sup> Increased early implant micromotion leads to the formation of peri-implant fibrous tissue, a decrease in osseointegration, and ultimately impaired long-term implant survival.<sup>2-5</sup> Implant instability manifests radiologically as subsidence, radiolucency, and the formation of a pedestal, a new shelf of bone at the distal tip of the implant indicating distal load transfer.<sup>6,7</sup> High initial implant micromotion negatively influences osseointegration by applying shear stress on bone cells, influencing their activation and differentiation, and impacting the vitality of osteoblasts and osteoclasts.<sup>3,8</sup>

Intermittent administration of parathyroid hormone (iPTH) has an anabolic effect on bone formation by increasing osteoblast differentiation, inhibiting osteoblastic apoptosis, and activating lining cells.<sup>9-11</sup> Multiple studies have shown a beneficial effect of PTH treatment on osseointegration;<sup>12-14</sup> however, most studies have been conducted on press-fit implantation without loading conditions, and have not explored the capacity of iPTH to restabilize initial unstable implants and the influence of the progression of peri-implant fibrous tissue.

In this study, we developed a murine model with initial implant instability and explored whether iPTH treatment administration at two clinically relevant timepoints (immediately postoperatively or after acute presentation of loose implantation) can prevent and prohibit the formation of peri-implant fibrosis while mediating osseointegration. Additionally, we conducted a time course experiment analyzing the progression of osseointegration with iPTH treatment (Figure 1) to study the cell identity at the bone-implant interface.

### Methods

**Animals and surgical procedure.** This study was approved by the local Institutional Animal Care and Use Committee,

and we have included an ARRIVE checklist to show that we have conformed to the ARRIVE guidelines.

A total of 54 16-week-old C57Bl/6 mice (Jackson Laboratory, USA) were used for cementless implantation of a 3D laser-printed tibial prosthesis with a rough surface finish (Eosint M 270; Eos Electro Optical Systems, Germany) in the right knee joint. Figure 1 provides an overview of the study protocol. After surgery, the mice were randomly assigned to one of three groups. The first group (n = 22, phosphate buffered saline (PBS)-control group) received subcutaneous PBS (CORNING cellgro, USA; 1 ml/mouse 6 days/week) for four weeks post-implantation. The second group (n = 19; immediate iPTH) received 40 µg/kg of iPTH<sup>14</sup> (Bachem, USA) for six days per week subcutaneously for four weeks. A third group (n = 13; delayed iPTH) received PBS treatment for the first two weeks postoperatively, and then iPTH treatment for two weeks was initiated using the same dosing regimen as first iPTH group; four-week PBS-treated mice served as the controls for this experiment. Injections with either iPTH or PBS were performed until the day of euthanasia.

The surgical procedure has been previously described in detail.<sup>14</sup> For overdrill experimental groups, a 1.4 mm (155% oversized) drill-hole was used to permit micromotion. A titanium implant with a 1.0 mm porous-coated stem diameter was inserted into the oversized intramedullary canal. After insertion the tibial implant was completely unstable (Supplementary Video 1). After reduction of the patella, the extensor mechanism was closed with resorbable sutures, and skin closure was performed with a non-resorbable suture material. Analgesics were administered for three postoperative days as per institutional guidelines.

Peri-implant cell composition was observed over four weeks via histological analysis: mice from iPTH and PBS-control groups were euthanized at one-week (n = 3/group), two-week (n = 3/group), and four-week (n = 3/group) timepoints, and mice from the delayed treatment group were euthanized four weeks (n = 3) post-implantation. Four weeks postoperatively, mice from all three groups (n = 10/group) were euthanized and analyzed via micro-CT (µCT) followed by pull-out testing.

**Radiological analysis.** Radiographs were obtained one, two, and four weeks post-implantation using a high-resolution digital radiography system (UltraFocus, Faxitron, USA). Inhalation anaesthetics (2% isoflurane, 2 l/min) were used to minimize movement during the radiological assessment. The mouse was placed in prone position and the right hip and knee were put in a slightly flexed position. Radiographs were analyzed using imaging processing software (BiopticsVision, USA).

**Histological assessments.** Previously described methods for haematoxylin and eosin (H&E) and immunofluorescence (IF) staining were used.<sup>15</sup> Briefly, the right tibiae were dissected from skin and soft-tissue. Samples were fixed in 4% ice-cold paraformaldehyde for four hours and then decalcified using 0.5 M ethylenediamine-tetraacetic acid (EDTA) at 4°C under constant shaking.

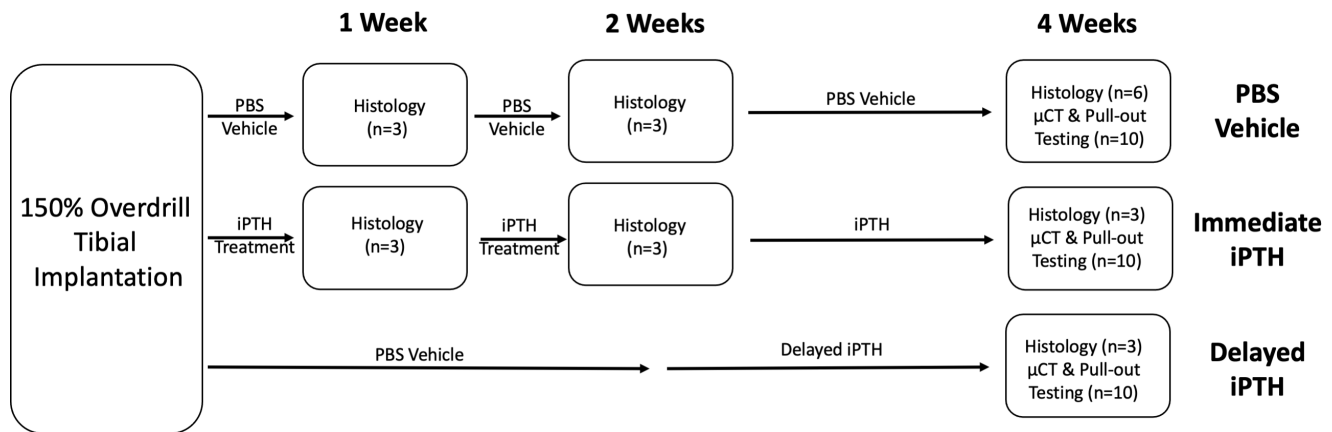


Fig. 1

Outline of the experimental design of the study. iPTH, intermittent parathyroid hormone; PBS, phosphate buffered saline;  $\mu$ CT, micro-CT.

Cryoprotection was carried out in ice-cold 20% sucrose solution overnight. Prior to embedding, the implants were gently removed from the implantation site. Under a high-magnification microscope, no residual tissue was observed on the extracted implant, confirming that our protocol for implant removal did very little to disrupt the bone-implant interface. All samples were embedded in optimal cutting temperature (OCT; Sakura, USA) and cut in sagittal sections using a cryostat (Leica Biosystems, USA).

Samples were cut in 10  $\mu$ m thick sections, dehydrated by using a series of ethanol washes, cleared in xylene, stained with H&E or picrosirius red, and mounted with xylene-based mounting medium. H&E and picrosirius red staining were conducted to assess the gross morphology of the peri-implant tissue. Stained slides were visualized using a light microscope with polarized light capabilities (Eclipse E800; Nikon, Japan). Picrosirius red staining was used to distinguish between bone and fibrous tissue formation through tissue birefringence under polarized light microscopy.<sup>16,17</sup> The stained tissues sections were placed at 0°, a prism to polarize the light was rotated 45°, and images were obtained.

For IF, the fixed, decalcified, and cryoprotected tibiae were embedded in OCT and 20  $\mu$ m-thick sagittal slices were cut. Sections were rehydrated with PBS, permeabilized with 0.3% Triton X solution (MilliporeSigma, USA), and after subsequent washes with PBS, blocked with 5% donkey serum (MilliporeSigma). Sections were then treated with primary antibodies and incubated at 4°C overnight. The following primary antibodies have been used in this study: anti-endomucin (1:100; SC65495, Santa Cruz Biotech, USA), anti-osteopontin (OPN) (1:100, AF808, R&D Systems, USA), anti-osterix (OSX) (1:100, AB209484, Abcam, UK), anti-platelet-derived growth factor receptor  $\alpha$  (PDGFR $\alpha$ ) (1:100, AB69569, Abcam), and anti-PU.1 (1:100, 22585, Cell Signaling, USA). Primary antibodies were visualized with species-appropriate Alexa Fluor-coupled secondary antibodies (1:400; Thermo Fisher Scientific, USA). Nuclei were counterstained with

4,6-diamidino-2-phenylindole (DAPI) (1:10.000, Thermo Fisher Scientific). All IF images were acquired by using a Zeiss LSM-880 confocal microscope (Carl Zeiss Microscopy GmbH, Germany). Image processing was obtained using Zeiss Zen Black software (Carl Zeiss Microscopy GmbH) and ImageJ software (National Institutes of Health and the Laboratory for Optical and Computational Instrumentation (LOCI), University of Wisconsin–Madison, USA).

**Biomechanical assessment.** Pull-out testing of the tibial implant was performed to assess implant stability. Tibiae from the iPTH, PBS-control, and delayed iPTH groups (n = 10/group) were collected four weeks post-implantation. The distal tibia and diaphysis were potted in polymethylmethacrylate (PMMA)<sup>14</sup> and tested with an EnduraTEC ELF 3200 system (Bose, USA). Implants were pulled out at 0.03 mm/sec under displacement of failure. Maximum pull-out load in Newtons (N) was calculated from the obtained load-displacement curves.

**Micro-CT.** Scans ( $\mu$ CT 35, Scanco Medical, Switzerland) were performed at 6  $\mu$ m voxel size, 55 kVp, 145 mA, and 0.36 rotation step (180 angular range) per view. Image acquisition was performed on samples obtained from the PBS-control, iPTH, and delayed iPTH treatment groups at four weeks after surgery (n = 10/group). Regions of interest were defined as peri-implant (cancellous bone 500  $\mu$ m around the distal parts of the stem) and distal to implant (cancellous bone 500  $\mu$ m distal from the tip of the stem). This method was chosen to include just the tibial metaphysis and to exclude the growth plate. Radiological bone morphological parameters, particularly bone volume fraction (bone volume/total volume; BV/TV), trabecular number, trabecular thickness, and trabecular separation were assessed.

**Statistical analysis.** All data from the biomechanical assessment and  $\mu$ CT-analyses are reported as mean (standard deviation (SD)). All analyses with three groups in comparison (PBS, immediate iPTH and delayed iPTH) were conducted using a one-way analysis of variance (ANOVA), and for analyses with two groups in comparison (PBS and

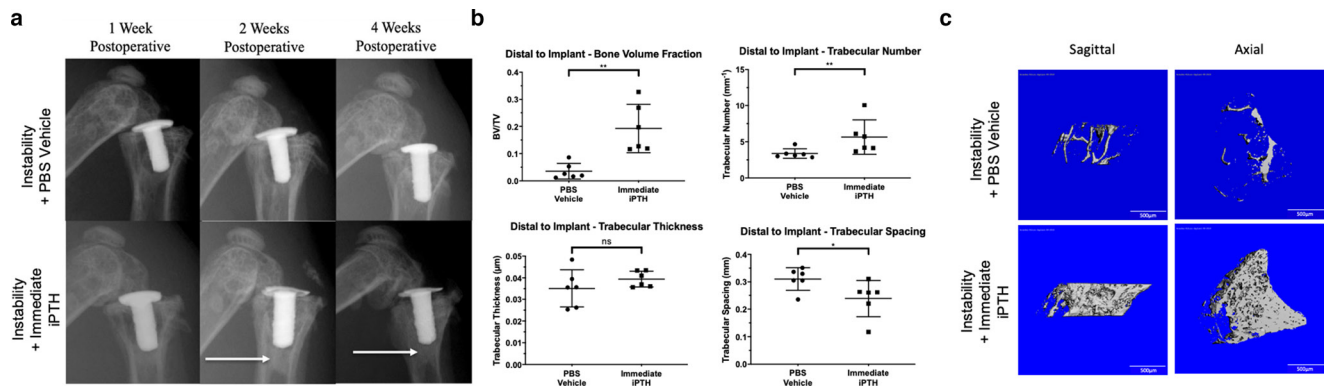


Fig. 2

a) Radiological and b) to c) micro-CT ( $\mu$ CT) comparison of implant instability treated with either phosphate buffered saline (PBS)-control or intermittent parathyroid hormone (iPTH). After one week, both groups showed distinct signs of radiolucency around the implant. A distinct reduction of radiolucent lines can be seen in the iPTH group over time. Both groups exhibited the formation of a pedestal sign (white arrow); b) to c)  $\mu$ CT measurements of pedestal-sign trabecular bone after four weeks of PBS-control or iPTH treatment (\* $p < 0.05$ , \*\* $p < 0.01$ , \*\*\* $p < 0.001$ ). Scale bars = 500  $\mu$ m. BV/TV, bone volume fraction; ns, not significant.

immediate iPTH) an independent-samples *t*-test was performed. All statistics were performed on GraphPad Prism 8 (GraphPad Software, USA) and SPSS 28.0 (IBM, USA). Kolmogorov–Smirnov test was applied to test for normal distribution and revealed a normal distribution for all parametric data in this study (pull-out strength:  $p = 0.189$ ; BV/TV distal to implant:  $p = 0.104$ ; BV/TV peri-implant:  $p = 0.183$ ). Statistical significance was set at  $p < 0.05$ .

## Results

This murine overdrill-model demonstrated peri-implant radiolucencies with distinct bone formation at the distal tip of the implant consistent with a pedestal sign formation, two hallmark signs of loosening observed clinically (Figure 2a). After four weeks of iPTH treatment, mean distal-to-implant BV/TV increased five-fold when compared to control, an increase of 0.19 (SD 0.09) vs 0.04 (SD 0.03) ( $p = 0.01$ , independent-samples *t*-test). iPTH treatment also significantly increased distal-to-implant trabecular number and decreased trabecular spacing, while retaining trabecular thickness (Figures 2b and 2c)

After four weeks, PBS-control mice exhibited robust fibrous tissue encapsulation at the peri-implant region with a thin pedestal consistent with the clinical presentation of patients undergoing aseptic loosening revision surgery. iPTH-treated mice, on the other hand, developed bone at the pedestal and peri-implant bone through four weeks without the presence of fibrous tissue (Figure 3).

Observational histology revealed that iPTH treatment seemed to increase osteoblast differentiation and osteocytes (indicated by OSX and OPN, respectively) in the peri-implant region and pedestal and cortical bone (Figure 4a). iPTH apparently induced angiogenesis as observed through endomucin (EMCN) vascular endothelium cells in the peri-implant and pedestal trabecular bone over time (Figure 4b). Pro-fibrotic fibroblasts (platelet-derived growth factor receptor  $\alpha$  positive (PDGFR $\alpha^+$ ) and PU.1 $^+$ ) encapsulated the implant with PBS-control (Figure 5).

This treatment eliminated radiolucencies (Figure 6a), induced robust peri-implant bone formation, and prohibited the progression of fibrous tissue around the implant (Figure 6b). These observational findings were accompanied by an increase in osteoblasts and vasculature endothelium up to the implant and in the pedestal with iPTH treatment (Figure 6c). Few to no pro-fibrotic fibroblast (PDGFR $\alpha^+$ , PU.1 $^+$ ) cells could be detected at the implant interface with PTH treatment (Figure 6d).

Immediate and delayed iPTH treatment both increased peri-implant trabecular bone compared to PBS-control treatment (Figure 7a). Four weeks of treatment with PBS-control resulted in a mean peri-implant BV/TV of 0.23 (SD 0.03), while immediate and delayed iPTH treatment increased mean BV/TV to 0.46 (SD 0.07) and 0.34 (SD 0.10), respectively (Figure 7b) (PBS-control vs immediate iPTH,  $p < 0.001$ ; PBS-control vs delayed iPTH,  $p = 0.048$ ; immediate iPTH vs delayed iPTH,  $p = 0.111$ ). iPTH treatment increased the mean force required to pull out the implant from 8.41 N (SD 8.15) in the PBS-control group to 21.49 N (SD 10.45) and 23.68 N (SD 8.99) in the immediate and delayed iPTH treatment groups, respectively (PBS-control vs immediate iPTH,  $p = 0.023$ ; PBS-control vs delayed iPTH,  $p = 0.002$ ; immediate iPTH vs delayed iPTH,  $p = 0.347$ ).

## Discussion

Inadequate initial implant fixation after arthroplasty is a major contributor to aseptic joint arthroplasty failure.<sup>1</sup> In this study, we present the positive effects of immediate and delayed iPTH treatment on peri-implant bone formation and implant fixation in a clinically representative murine model of instability. These findings are the first to demonstrate that iPTH can treat initial implant instability, effectively promoting osseointegration and preventing the progression to aseptic loosening.

Multiple studies have shown positive effects of iPTH treatment on osseointegration.<sup>12,14,18-21</sup> However, these



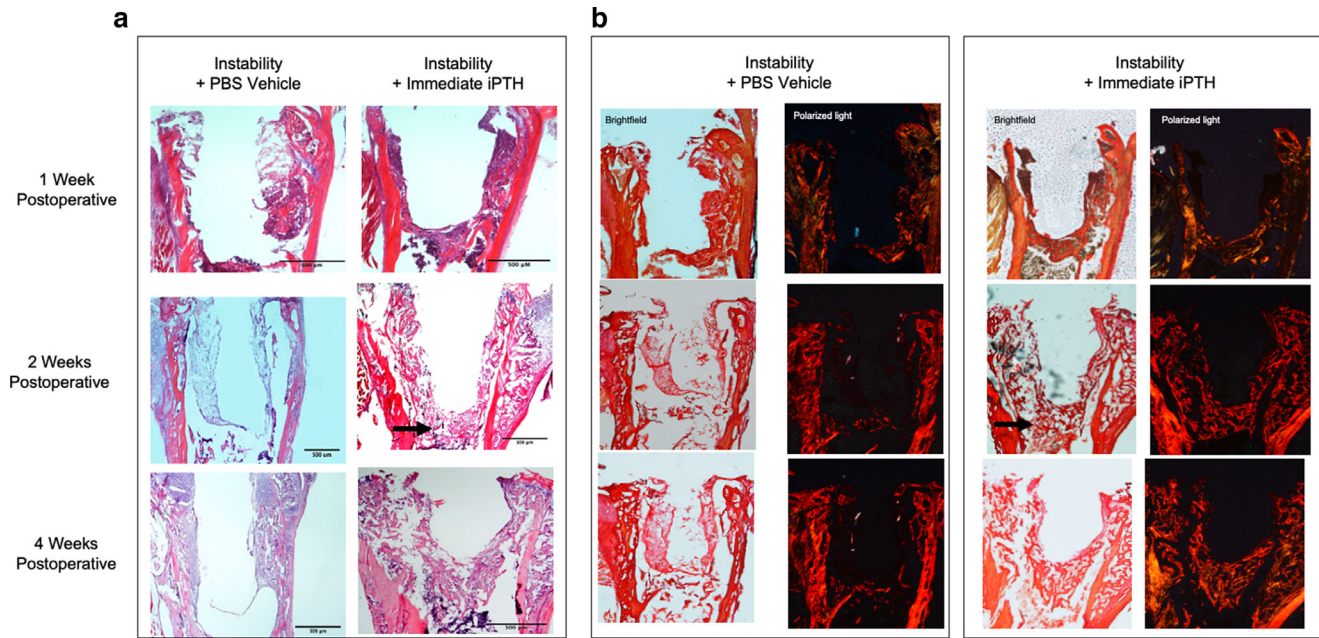


Fig. 3

a) Histological assessment of implant instability treated with phosphate buffered saline (PBS)-control or intermittent parathyroid hormone (iPTH) through haematoxylin and eosin staining. Both groups displayed minimal peri-implant bone formation after one week post-treatment. After two weeks of treatment, the PBS-control group still showed minimal bone formation but a clear fibrous tissue formation is visible, whereas in the iPTH-treated group, enhanced intramembranous bone formation (arrow, also shown in Fig. 3b) and a clear pedestal at the distal tip are seen. b) Through picrosirius red staining, it is possible to show differences in the collagen composition between peri-implant bone and fibrous tissue formation within the two treatment groups. Scale bars = 500 µm.

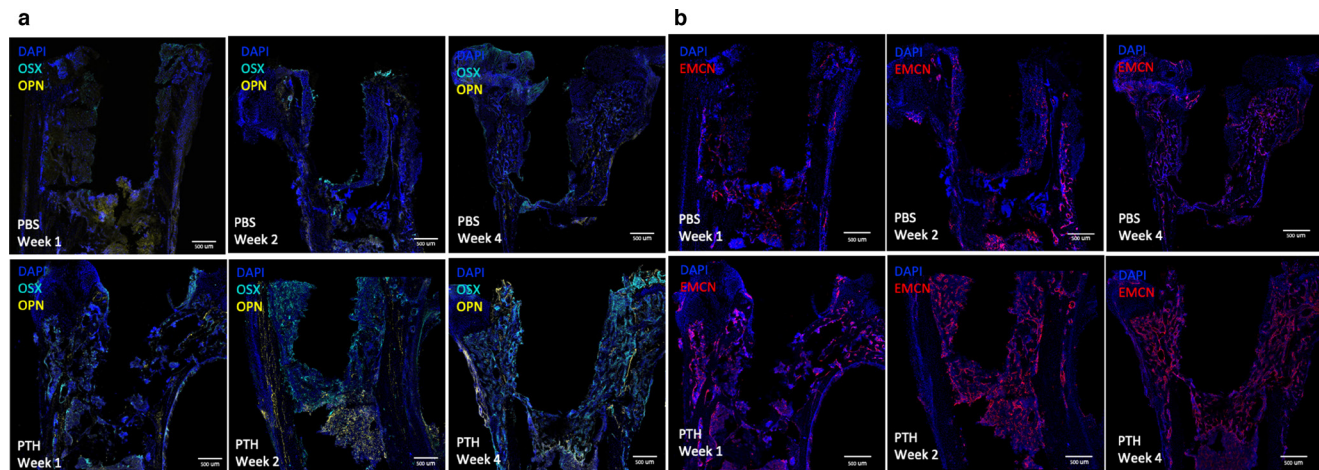


Fig. 4

Immunofluorescence staining of phosphate buffered saline (PBS)-control and intermittent parathyroid hormone (iPTH) treatment. a) Minimal progression of peri-implant bone formation is present in the PBS-control group, whereas after two weeks and four weeks of iPTH treatment increases in osterix (OSX), osteopontin (OPN) at distal pedestal region, and b) endomucin (EMCN) expression are detected, indicating angiogenesis around the implant with osseointegration. Scale bars = 500 µm. DAPI, 4,6-diamidino-2-phenylindole.

reports often observe iPTH treatment with press-fit implantation<sup>14,18-21</sup> in areas unrelated to arthroplasty (extra-articular and additional stability through cortical bone) without loading conditions.<sup>12,20</sup> In our model, oversizing the drill-hole to 150% of the stem-diameter effectively results in radiological signs of implant loosening. As seen clinically, we observed radiolucent lines, subsidence, and the formation of a pedestal sign at the distal tip

of the implant, indicating implant instability. iPTH treatment, however, led to a distinct prevention or reversal of these features. Our findings confirm the reports from Engh et al,<sup>7</sup> which suggest that radiolucency and a distal pedestal represent distinct signs of an unstable implant. It is hypothesized that the pedestal forms at the distal tip of the implant to support and stabilize the implant in this area.<sup>22</sup> This theory is supported by our histological and

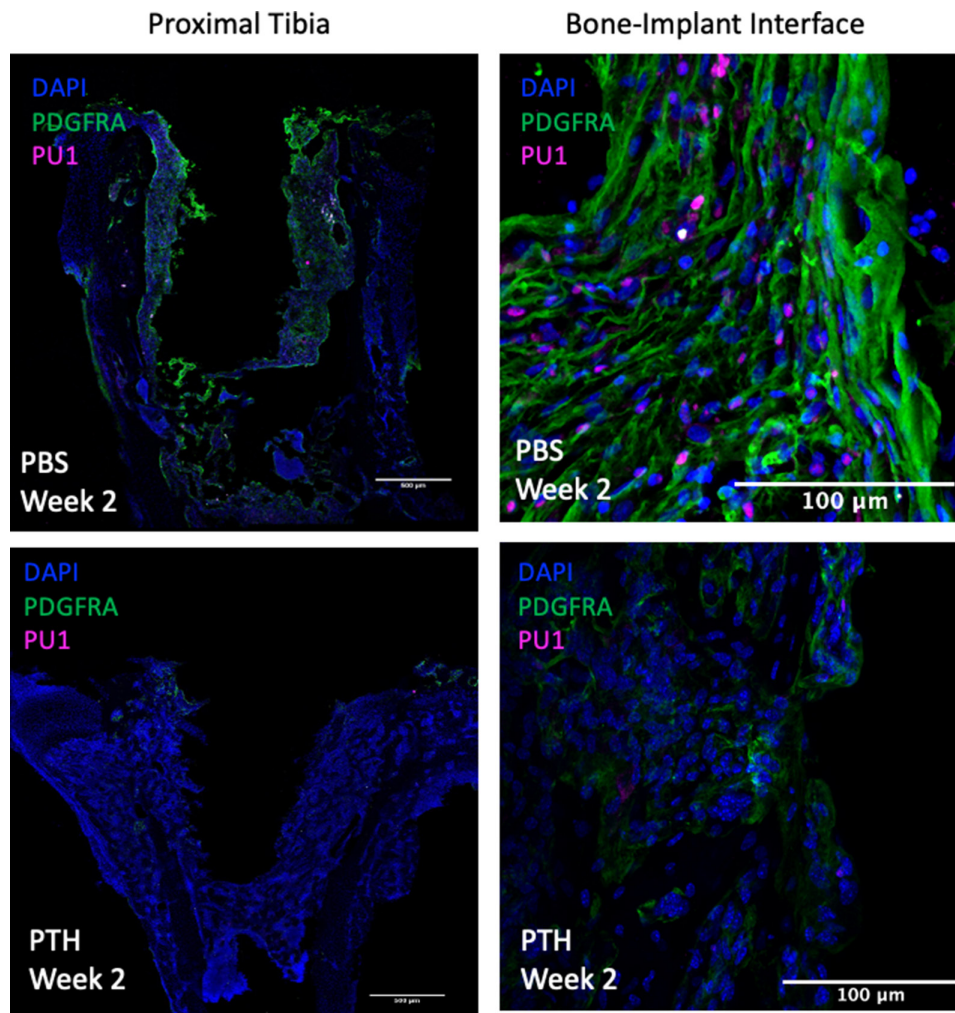


Fig. 5

Membrane formation visualized through immunofluorescence staining with platelet-derived growth factor receptor  $\alpha$  (PDGFRA) and PU.1 labelling. The intermittent parathyroid hormone (iPTH)-treated group displays a distinct decrease in PDGFRA and PU.1 signal, indicating a reduction of fibrous tissue formation around the implant. Scale bars: 500  $\mu\text{m}$  (left panel) and 100  $\mu\text{m}$  (right panel). DAPI, 4,6-diamidino-2-phenylindole.

$\mu\text{CT}$  findings, where iPTH-treated groups showed a 475% higher trabecular BV/TV at the distal tip of the implant compared to the PBS-control group.

Aseptic loosening is associated with peri-implant fibrous tissue formation,<sup>2,3,23-26</sup> and early increased implant micromotion has been shown to result in fibrous tissue development around the implant.<sup>27</sup> Duyck et al<sup>4</sup> showed that micromotions exceeding 30  $\mu\text{m}$  lead to impaired osseointegration and fibrous tissue formation. According to our findings, it appears that iPTH treatment induces a cellular and molecular change at the peri-implant interface with less fibrous tissue formation and increased bone formation. However, further studies are needed to confirm these findings. Despite using a wear-particle induced aseptic loosening model that is distinct from the model used in this study, Hu et al<sup>23</sup> found that

iPTH treatment alone and a combination treatment with bisphosphonates led to increased implant stability.

When patients present clinically with a loose implant, the fibrous tissue has already been established between the bone-implant interface. To investigate the therapeutic potential of iPTH in this scenario, we explored delaying iPTH treatment. In our model, delayed iPTH treatment was still able to prohibit the progression of fibrous tissue and enhance peri-implant bone formation. To assess the functional difference at the bone-implant interface associated with these different cell populations,  $\mu\text{CT}$  and biomechanical testing were conducted. Biomechanical findings confirmed that iPTH stabilizes the loose implant, indicating that even a delayed onset of iPTH treatment may have beneficial effects on the osseointegration of an unstable implant. Interestingly, both iPTH-treated groups exhibited pull-out forces compared to regular press-fit



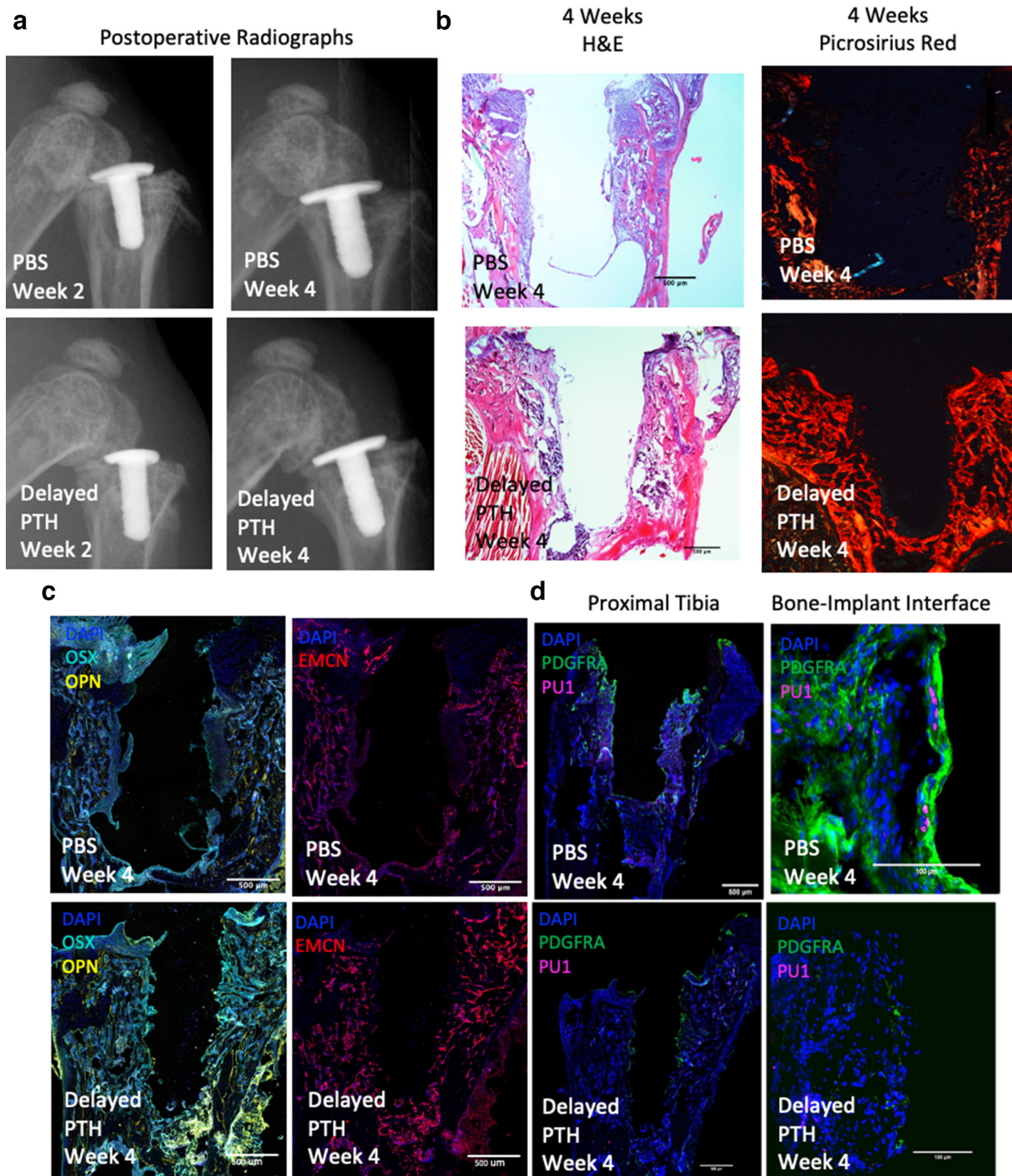


Fig. 6

a) Radiological analysis shows distinct signs of implant instability after two weeks of phosphate buffered saline (PBS)-control. However, initiating intermittent parathyroid hormone (iPTH) after two weeks (delayed iPTH treatment) was still sufficient to enhance bone formation and reduce radiolucency. Scale bars = 500  $\mu$ m. b) Radiological findings and reduction of fibrous tissue formation are confirmed through haematoxylin and eosin and picosirius red staining. Scale bars = 500  $\mu$ m. c) With iPTH treatment, it was still possible to enhance bone formation around the implant, as shown by immunofluorescence (IF)-staining visualization including labelling with 4,6-diamidino-2-phenylindole (DAPI), osterix (OSX), osteopontin (OPN), and endomucin (EMCN). Scale bars = 500  $\mu$ m. d) It was also possible to simultaneously inhibit the progression of peri-implant fibrous tissue formation by reducing platelet-derived growth factor receptor  $\alpha$  (PDGFR $\alpha$ ) and PU.1 positive cells. Scale bars: 500  $\mu$ m (left panel) and 100  $\mu$ m (right panel).

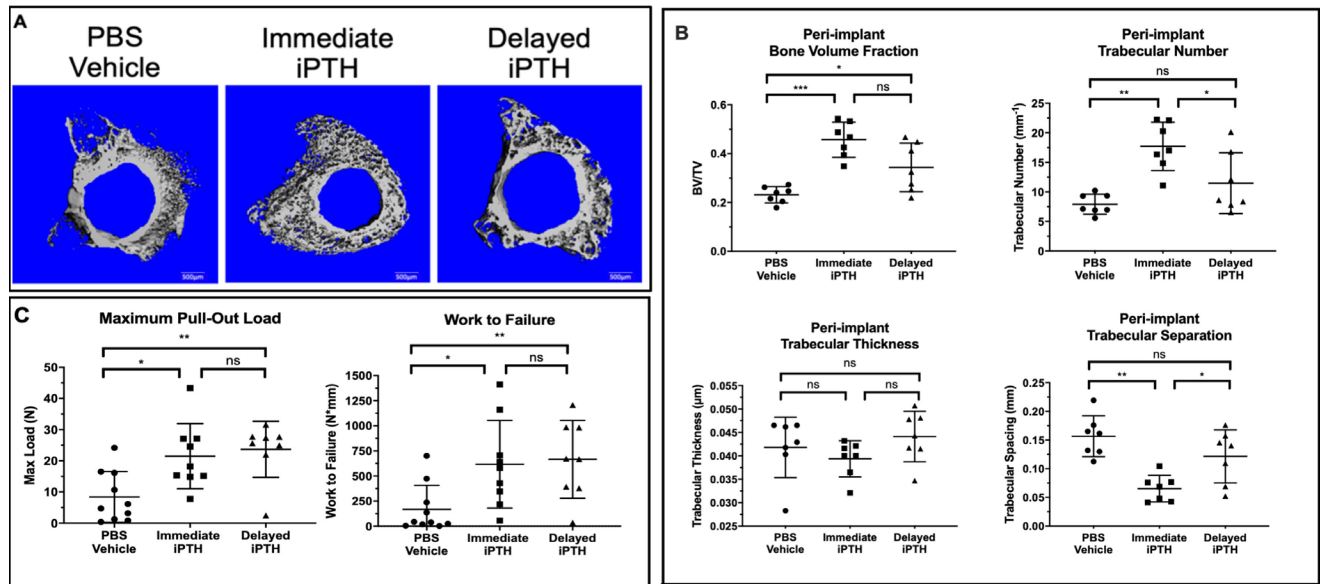


Fig. 7

Assessment of osseointegration via micro-CT ( $\mu$ CT) and biomechanical testing after four weeks of phosphate buffered saline (PBS)-control, immediate intermittent parathyroid hormone (iPTH), or delayed iPTH treatment. a) 3D  $\mu$ CT-reconstruction of peri-implant trabecular bone. Scale bar = 500  $\mu$ m. b)  $\mu$ CT analysis shows a significant increase in peri-implant bone formation with immediate and delayed administration of iPTH. c) Mean maximum load to pull-out was significantly increased with immediate and delayed iPTH treatment (\* $p < 0.05$ , \*\* $p < 0.01$ , \*\*\* $p < 0.001$ ). BV/TV, bone volume fraction; ns, not significant.

implantation, which were reported in another study from our study group.<sup>14</sup>

The origin and composition of peri-implant fibrous tissue still remains unclear. PDGFR $\alpha$ <sup>+</sup> mesenchymal progenitors have shown to be a major contributor to fibrosis in other organ systems (e.g. muscle, liver, heart)<sup>28-30</sup> by increasing extracellular matrix deposition. Blocking PDGFR $\alpha$ -signalling has been shown to have a beneficial effect on the inhibition of fibrosis.<sup>31</sup> Transcription factor PU.1 is highly expressed in macrophages and myeloid cells;<sup>32,33</sup> however, recent evidence indicates that upregulation of PU.1 also leads to an induction of pro-fibrotic gene expression resulting in enhanced extracellular matrix deposition by fibroblasts.<sup>34</sup> In a recent study, our group was able to show an abundance of PDGFR $\alpha$ <sup>+</sup> PU.1<sup>+</sup> cells in interfacial fibrous tissue from patients undergoing revision surgery due to non-wear particle induced aseptic loosening. However, further research is needed to confirm these findings. Our data suggest that iPTH treatment augments PU.1 fibroblast polarization in PDGFR $\alpha$ <sup>+</sup> cells, allowing for anabolic bone growth despite instability.

Our data show that iPTH induces osteoblastogenesis, as shown through OSX and OPN expression.<sup>35</sup> OPN cells were abundant at the pedestal and cortical bone, suggesting that this area is critical in stabilizing the implant and assisting in achieving osseointegration. Additionally, iPTH led to peri-implant angiogenesis as indicated through EMCN, a marker highly expressed in bone-specific Type H vessels.<sup>36-38</sup> The change in peri-implant cellular composition and bone formation increased osseointegration, exhibited by enhanced implant mechanical

strength, showing that delayed treatment can 'rescue' initial implant instability (Figure 7c).

Our study has some limitations. First, the histological/immunohistochemical results only provide a qualitative insight into the pathogenesis in our model, but future studies will employ quantitative strategies to analyze the immunophenotype and transcriptome of the peri-implant bone tissue.

Second, as mentioned earlier, the mechanism of initially unstable implants as presented here might not reflect the mechanism of long-term loosening due to wear, but this problem seems to be diminished with the use of contemporary polyethylenes,<sup>39</sup> and modern 3D-printed implant coatings and designs might reduce the risk of initially unstable implants.<sup>40</sup>

Translationally, our data suggest that iPTH can directly influence osseointegration at the bone-implant interface for patients with an initially unstable implant. If insufficient metaphyseal fill is observed intraoperatively and inadequate initial implant instability is suspected, iPTH treatment may prevent peri-implant fibrous tissue formation and long-term osseointegration failure. Additionally, if implant instability is suspected at an early follow-up visit, patients may benefit from iPTH treatment to resolve bone-implant fibrous tissue and increase peri-implant bone formation by reverting peri-implant cells to osteoblast-lineage cells. If iPTH treatment is authorized for the treatment of implant instability, patients with normal bone density need to be surveilled regularly, and informed about potential side effects of the treatment (e.g. hypercalcemia). Understanding the cell lineages responsible for osseointegration failure and



their response to PTH treatment will assist in identifying novel targeted therapeutics that inhibit aberrant cellular and molecular mechanisms driving osseointegration failure.

## Twitter

Follow K. Staats @kevinstaats

Follow B. R. Sosa @BrandenSosa1

Follow the authors @HSpecialSurgery

## Supplementary material



Video showing that overdrilling the tibia by 150% of the original stem size creates distinct signs of implant instability. An ARRIVE checklist is also included to show that the ARRIVE guidelines were adhered to in this study.

## References

- Streit MR, Haeussler D, Bruckner T, et al. Early migration predicts aseptic loosening of cementless femoral stems: a long-term study. *Clin Orthop Relat Res*. 2016;474(7):1697–1706.
- Jakobsen T, Kold S, Shiguetomi-Medina J, Baas J, Soballe K, Rahbek O. Topical zoledronic acid decreases micromotion induced bone resorption in a sheep arthroplasty model. *BMC Musculoskelet Disord*. 2017;18(1):441.
- Ziebart J, Fan S, Schulze C, Kämmerer PW, Bader R, Jonitz-Heincke A. Effects of interfacial micromotions on vitality and differentiation of human osteoblasts. *Bone Joint Res*. 2018;7(2):187–195.
- Duyck J, Vandamme K, Geris L, et al. The influence of micro-motion on the tissue differentiation around immediately loaded cylindrical turned titanium implants. *Arch Oral Biol*. 2006;51(1):1–9.
- Jasty M, Bragdon C, Burke D, O'Connor D, Lowenstein J, Harris WH. In vivo skeletal responses to porous-surfaced implants subjected to small induced motions. *J Bone Joint Surg Am*. 1997;79-A(5):707–714.
- Chang CY, Huang AJ, Palmer WE. Radiographic evaluation of hip implants. *Semin Musculoskelet Radiol*. 2015;19(1):12–20.
- Engh CA, Massin P, Suthers KE. Roentgenographic assessment of the biologic fixation of porous-surfaced femoral components. *Clin Orthop Relat Res*. 1990;257:107–128.
- Stadelmann VA, Terrier A, Pioletti DP. Microstimulation at the bone–implant interface upregulates osteoclast activation pathways. *Bone*. 2008;42(2):358–364.
- Silva BC, Bilezikian JP. Parathyroid hormone: anabolic and catabolic actions on the skeleton. *Curr Opin Pharmacol*. 2015;22:41–50.
- Jilka RL. Molecular and cellular mechanisms of the anabolic effect of intermittent PTH. *Bone*. 2007;40(6):1434–1446.
- Kim SW, Pajevic PD, Selig M, et al. Intermittent parathyroid hormone administration converts quiescent lining cells to active osteoblasts. *J Bone Miner Res*. 2012;27(10):2075–2084.
- Daugaard H, Elmengaard B, Andreassen T, Bechtold J, Lamberg A, Soballe K. Parathyroid hormone treatment increases fixation of orthopedic implants with gap healing: a biomechanical and histomorphometric canine study of porous coated titanium alloy implants in cancellous bone. *Calcif Tissue Int*. 2011;88(4):294–303.
- Li YF, Li XD, Bao CY, Chen QM, Zhang H, Hu J. Promotion of peri-implant bone healing by systemically administered parathyroid hormone (1-34) and zoledronic acid adsorbed onto the implant surface. *Osteoporos Int*. 2013;24(3):1063–1071.
- Yang X, Ricciardi BF, Dvorzhinskiy A, et al. Intermittent parathyroid hormone enhances cancellous osseointegration of a novel murine tibial implant. *J Bone Joint Surg Am*. 2015;97-A(13):1074–1083.
- Xu R, Yallowitz A, Qin A, et al. Targeting skeletal endothelium to ameliorate bone loss. *Nat Med*. 2018;24(6):823–833.
- Rittié L. Method for Picrosirius Red-Polarization Detection of Collagen Fibers in Tissue Sections. In: Rittié L, ed. *Fibrosis. Methods in Molecular Biology*. Vol 1627. Humana Press: New York, New York, 2017: 395–407.
- Ma R, Schär M, Chen T, et al. Use of human placenta-derived cells in a preclinical model of tendon injury. *J Bone Joint Surg Am*. 2019;101-A(13):e61.
- Daugaard H, Elmengaard B, Andreassen TT, Baas J, Bechtold JE, Soballe K. The combined effect of parathyroid hormone and bone graft on implant fixation. *J Bone Joint Surg Br*. 2011;93-B(1):131–139.
- Fahlgren A, Yang X, Ciani C, et al. The effects of PTH, loading and surgical insult on cancellous bone at the bone-implant interface in the rabbit. *Bone*. 2013;52(2):718–724.
- Rybaczek T, Tangl S, Dobsak T, Gruber R, Kuchler U. The effect of parathyroid hormone on osseointegration in insulin-treated diabetic rats. *Implant Dent*. 2015;24(4):392–396.
- Jiang L, Zhang W, Wei L, et al. Early effects of parathyroid hormone on vascularized bone regeneration and implant osseointegration in aged rats. *Biomaterials*. 2018;179:15–28.
- Vresilovic EJ, Hozack WJ, Rothman RH. Radiographic assessment of cementless femoral components. *J Arthroplasty*. 1994;9(2):137–141.
- Hu B, Wu H, Shi Z, et al. Effects of sequential treatment with intermittent parathyroid hormone and zoledronic acid on particle-induced implant loosening: evidence from a rat model. *J Orthop Res*. 2019;37(7):1489–1497.
- Mandelin J, Li TF, Hukkanen M, et al. Interface tissue fibroblasts from loose total hip replacement prosthesis produce receptor activator of nuclear factor-kappaB ligand, osteoprotegerin, and cathepsin K. *J Rheumatol*. 2005;32(4):713–720.
- Goldring SR, Schiller AL, Roelke M, Rourke CM, O'Neil DA, Harris WH. The synovial-like membrane at the bone-cement interface in loose total hip replacements and its proposed role in bone lysis. *J Bone Joint Surg Am*. 1983;65-A(5):575–584.
- De Man FHR, Tigchelaar W, Marti RK, Van Noorden CJF, Van der Vis HM. Effects of mechanical compression of a fibrous tissue interface on bone with or without high-density polyethylene particles in a rabbit model of prosthetic loosening. *J Bone Joint Surg Am*. 2005;87-A(7):1522–1533.
- Kuyl EV, Shu F, Sosa BR, et al. Inhibition of PAD4 mediated neutrophil extracellular traps prevents fibrotic osseointegration failure in a tibial implant murine model: an animal study. *Bone Joint J*. 2021;103-B(7 Supple B):135–144.
- Gallini R, Lindblom P, Bondjers C, Betsholtz C, Andrae J. PDGF-A and PDGF-B induces cardiac fibrosis in transgenic mice. *Exp Cell Res*. 2016;349(2):282–290.
- Hayes BJ, Riehle KJ, Shimizu-Albergine M, et al. Activation of platelet-derived growth factor receptor alpha contributes to liver fibrosis. *PLoS One*. 2014;9(3):e92925.
- Uezumi A, Fukada S, Yamamoto N, et al. Identification and characterization of PDGFR $\alpha$  mesenchymal progenitors in human skeletal muscle. *Cell Death Dis*. 2014;5(4):e1186.
- Lemos DR, Babaeijandaghi F, Low M, et al. Nilotinib reduces muscle fibrosis in chronic muscle injury by promoting TNF-mediated apoptosis of fibro/adipogenic progenitors. *Nat Med*. 2015;21(7):786–794.
- Ross IL, Dunn TL, Yue X, Roy S, Barnett CJ, Hume DA. Comparison of the expression and function of the transcription factor PU.1 (Spi-1 proto-oncogene) between murine macrophages and B lymphocytes. *Oncogene*. 1994;9(1):121–132.
- Turkistany SA, DeKoter RP. The transcription factor PU.1 is a critical regulator of cellular communication in the immune system. *Arch Immunol Ther Exp (Warsz)*. 2011;59(6):431–440.
- Wohlfahrt T, Rauber S, Uebe S, et al. PU.1 controls fibroblast polarization and tissue fibrosis. *Nature*. 2019;566(7744):344–349.
- Nakashima K, Zhou X, Kunkel G, et al. The novel zinc finger-containing transcription factor osterix is required for osteoblast differentiation and bone formation. *Cell*. 2002;108(1):17–29.
- Wang L, Zhou F, Zhang P, et al. Human type H vessels are a sensitive biomarker of bone mass. *Cell Death Dis*. 2017;8(5):e2760.
- Ji G, Xu R, Niu Y, et al. Vascular endothelial growth factor pathway promotes osseointegration and CD31hiEMCNhi endothelium expansion in a mouse tibial implant model: an animal study. *Bone Joint J*. 2019;101-B(7 Supple C):108–114.
- Caire R, Roche B, Picot T, et al. Parathyroid hormone remodels bone transitional vessels and the leptin receptor-positive pericyte network in mice. *J Bone Miner Res*. 2019;34(8):1487–1501.
- Davis ET, Pagkalos J, Kopjar B. A higher degree of polyethylene irradiation is associated with a reduced risk of revision for aseptic loosening in total hip arthroplasties using cemented acetabular components: an analysis of 290,770 cases from the National Joint Registry of England. *Bone Joint Res*. 2020;9(9):563–571.
- Dall'Ava L, Hothi H, Henckel J, et al. Osseointegration of retrieved 3D-printed, off-the-shelf acetabular implants. *Bone Joint Res*. 2021;10(7):388–400.

### Author information:

- K. Staats, MD, PhD, Orthopaedic Surgeon, Researcher, Hospital for Special Surgery, New York City, New York, USA; Department of Orthopedics and Trauma Surgery, Medical University of Vienna, Vienna, Austria.
- B. R. Sosa, BS, Researcher
- E-V. Kuyl, BS, Researcher

- Y. Niu, MD, PhD, Researcher
- V. Suhardi, MD, PhD, Orthopaedic Surgeon
- K. Turajane, BS, Researcher
- L. Ivashkiv, MD, Researcher
- M. P. G. Bostrom, MD, Orthopaedic Surgeon
- X. Yang, MD, Researcher  
Hospital for Special Surgery, New York City, New York, USA.
- R. Windhager, MD, Head of Department, Department of Orthopedics and Trauma Surgery, Medical University of Vienna, Vienna, Austria.
- M. B. Greenblatt, MD, PhD, Assistant Professor, Department of Pathology and Laboratory Medicine, Weill Cornell Medical College, New York City, New York, USA.

**Author contributions:**

- K. Staats: Conceptualization, Data curation, Formal Analysis, Investigation, Methodology, Validation, Visualization, Writing – original draft, Writing – review & editing.
- B. R. Sosa: Conceptualization, Data curation, Formal Analysis, Investigation, Methodology, Validation, Visualization, Writing – original draft, Writing – review & editing.
- E-V. Kuyil: Investigation, Validation, Visualization, Writing – original draft, Writing – review & editing.
- Y. Niu: Conceptualization, Formal Analysis, Methodology, Project administration, Validation, Visualization.
- V. Suhardi: Conceptualization, Data curation, Investigation, Methodology, Validation, Visualization.
- K. Turajane: Formal Analysis, Investigation, Validation, Visualization.
- R. Windhager: Methodology, Project administration, Resources, Supervision, Writing – original draft, Writing – review & editing.
- M. B. Greenblatt: Conceptualization, Methodology, Project administration, Resources, Supervision, Writing – original draft, Writing – review & editing.

- L. Ivashkiv: Conceptualization, Methodology, Project administration, Resources, Supervision, Validation, Writing – original draft, Writing – review & editing.
- M. P. G. Bostrom: Conceptualization, Funding acquisition, Methodology, Project administration, Resources, Supervision, Validation, Writing – original draft, Writing – review & editing.
- X. Yang: Conceptualization, Funding acquisition, Investigation, Methodology, Project administration, Resources, Supervision, Validation, Writing – original draft, Writing – review & editing.
- K. Staats and B. R. Sosa contributed equally to this work.

**Funding statement:**

- The authors received no financial or material support for the research, authorship, and/or publication of this article.

**Ethical review statement:**

- This study was approved by the Institutional Animal Care and Use Committee (IACUC) of the Hospital For Special Surgery – Weill Cornell Medical College; Protocol number: 2016-0013.

**Open access funding**

- The authors report that the open access funding for their manuscript was self-funded.

© 2022 Author(s) et al. This is an open-access article distributed under the terms of the Creative Commons Attribution Non-Commercial No Derivatives (CC BY-NC-ND 4.0) licence, which permits the copying and redistribution of the work only, and provided the original author and source are credited. See <https://creativecommons.org/licenses/by-nc-nd/4.0/>